ELSEVIER

Journal of Nuclear Materials 273 (1999) 265–270

journal of nuclear materials

www.elsevier.nl/locate/jnucmat

Characterization of hydrogen permeation through recycled cast iron for subsurface disposal

A.M. Brass [a,*], F. Barbier [b]

[a] *Laboratoire de Métallurgie Structurale, CNRS URA 1107, Bât. 410, Université Paris-Sud, 91405 Orsay, France*
[b] *CEA-CEREM/SCECF, BP 06, 92265 Fontenay aux Roses, France*

Received 21 December 1998; accepted 18 February 1999

Abstract

The behavior of hydrogen in cast iron was investigated in order to assess the suitability of this material to be used in the near temperature range for the subsurface containment of radioactive wastes in which residual tritiated water may be present. The diffusion coefficient of hydrogen was determined in two different microstructures with the electrochemical permeation technique at room temperature, both from build up and degassing transients. In 0.1 N NaOH the hydrogen diffusivity ($1–4 \times 10^{-8}$ cm^2/s) and the steady state hydrogen flux at 298 K are markedly smaller in cast iron than in ferritic steels.

PACS: 25.40L; 82.80.Fk; 81.65.Kn

1. Introduction

Cast iron may be a candidate material for the storage of radioactive wastes due to its very good properties in corrosive atmospheres, for example in synthetic solutions representative of a concrete water [1], when compared to ferritic steels. The knowledge of the diffusivity of radioelements such as tritium which may be found in the wastes is necessary to characterize the performances of storage containers submitted to subsurface disposal environmental conditions. However although hydrogen is suspected to have an embrittling effect on ductile cast irons [2], the available data on the hydrogen (or its isotopes) diffusion coefficient in cast iron are very scarce and obtained by gas phase charging at high temperatures [3].

The purpose of this study was to assess the diffusivity of hydrogen produced by electrochemical means in cast iron at room temperature for comparison with the hydrogen behavior in concrete and in ferritic steels currently used for subsurface disposal.

The electrochemical permeation technique [4] was used to quantify the diffusion coefficient of hydrogen and the permeability of cast iron samples in an alkaline medium with a pH representative of the residual water encountered in the storage containers.

2. Material and experimental procedure

2.1. Material

Coupons were taken out of the wall of cast containers and then cut with a microcutting device. The containers were manufactured from recycled cast iron which was poured in specific ferritic steel moulds after melting at 1473 K. The chemical composition of the cast iron is given in Table 1. Samples were polished to diamond finish and a metallographic study was carried out to characterize the microstructure. Two sets of samples representative of the different microstructures found in the cast iron containers were selected for the permeation study.

Additional metallographic observations were performed by optical and scanning electron microscopy on the surface of specimens which was submitted to cathodic hydrogen charging in the permeation cell.

* Corresponding author.

0022-3115/99/$ – see front matter
PII: S0022-3115(99)00058-6

Table 1
Chemical composition of cast iron

Elements	C	Si	Mn	Cu	Cr	Ni	Fe
wt%	3.35	1.82	0.31	0.28	0.92	0.69	bal.

2.2. Permeation tests

The electrochemical permeation tests [4] were performed on 1 mm thick slices. The permeation cell is composed of two double wall glass compartments separated by the sample (working electrode) clamped in a separate sample holder. Water is circulated in the double jacket in order to maintain a constant temperature in each chamber (298 ± 0.5 K).

The flux of hydrogen diffusing through the sample cathodically polarized on one face (input face) is continuously measured on the other face (output face). The reduction of hydrogen in alkaline solutions proceeds according to: $2\,H_2O + 2e^- \rightarrow H_2 + 2\,OH^-$. The hydrogen atoms emerging on the output face are oxidized according to: $H_{ads} \rightarrow H^+ + e^-$. The hydrogen flux ($J$) is proportional to the anodic current detected on the output face with a detection threshold of about 4.9×10^{-15} mol H_2 cm^{-2} s^{-1}. A steady state regime is reached when the concentration gradient in the metallic sheet becomes linear.

The test is conducted as follows [5]: a preheated and deaerated 0.1 N NaOH solution is introduced in the anodic compartment of the cell where the rest potential of the specimen is measured for 15–16 h until stabilization. By polarizing the output surface at the rest potential value, a residual current density (background) less than 10 nA cm^{-2} is obtained. The hydrogen charging is then started by introducing the charging medium in the cathodic compartment under potentiostatic control. The tests were performed at −1350 mV/SCE in 0.1 N NaOH. Some experiments were also run at −800 mV/SCE in 0.1 N H_2SO_4.

When the steady state is reached, the cathodic polarization is interrupted by changing instantaneously the value of the applied potential from the cathodic value to 0 mV/SCE. The decay of the hydrogen flux can then be recorded continuously as a function of time on the output side of the sample. The desorption curve is representative of 'diffusible' hydrogen (lattice and weakly trapped hydrogen). Hydrogen in the 'deep' traps [6] is not released and degassing is achieved when the anodic current recovers the initial background value (a few nA/cm^2). Schematic permeation and degassing curves are represented in Fig. 1.

The time dependence of the dimensionless equation of the flux (J) normalized with respect to the stationary value (J_∞) is given by the Fick's law solutions for diffusion in a plane sheet of thickness L with a constant concentration of dissolved hydrogen on the input side of the sheet (C_o) [7]:

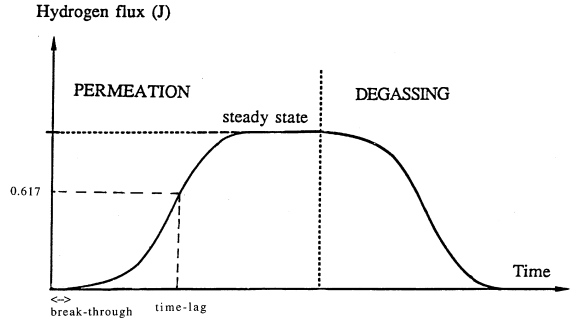

Fig. 1. Schematic permeation and degassing curves.

$$(J/J_\infty) = \frac{2}{\sqrt{\tau\pi}} \sum_{n=0}^{\infty} \exp\left[-\frac{(2n+1)^2}{4\tau}\right]$$
$$= 1 + 2\sum_{n=1}^{\infty} (-1)^n \exp(-n^2\pi^2\tau)$$

$\tau = D_l t/L^2$ is a dimensionless parameter, with D_l the lattice diffusion coefficient, t the time and L the sample thickness.

The diffusion coefficient of hydrogen is usually calculated with mathematical expressions derived from Fick's solutions for the appropriate boundary conditions: $D = L^2/at$, where a is a constant depending on the boundary conditions and on the time value chosen in the diffusion transient. In this work, both the time lag (tl) and the break through time (bt) [4,8,9] (Fig. 1) were chosen to calculate the apparent diffusion coefficient D in order to have an insight on changes that may occur if a purely Fickian diffusion process is not effective during the whole build up permeation transient. In the following, the steady state or maximum value of the hydrogen flux (J_∞) is normalized for a 1 cm thickness.

2.3. Cyclic voltammetry

The electrochemical behavior of the cast iron at 298 K was assessed by recording cyclic voltammograms at 0.55 mV/s in the non deaerated alkaline and acidic solutions. The potential was swept back and forth from the cathodic to the oxygen evolution region starting from −2000 mV/SCE in 0.1 N NaOH and from −1000 mV/SCE in 0.1 N H_2SO_4. The corrosion rates were computed from the Tafel slopes.

3. Results and discussion

3.1. Microstructural observations

The optical micrographs shown in Fig. 2 are representative of the two chosen microstructures. In one case (Fig. 2(a)) seldomly oriented graphite lamellae are

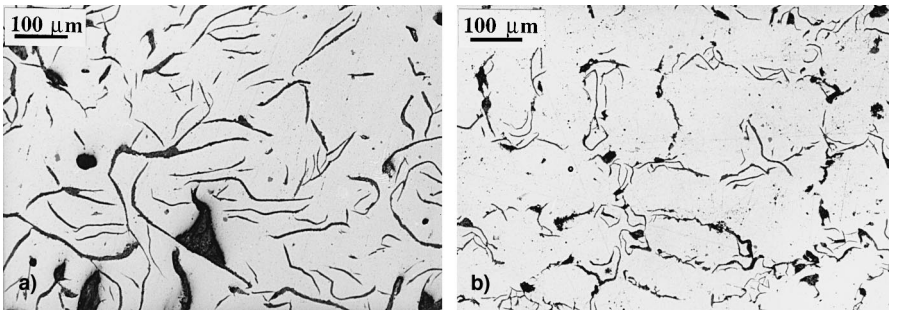

Fig. 2. Optical micrographs of the microstructure of cast iron: (a) seldomly oriented graphite lamellae, (b) oriented interdendritic graphite.

Table 2
Permeation characteristics of hydrogen in cast iron as a function of microstructure (0.1 N NaOH, −1350 mV/SCE, 298 K)

Microstructure	D_{bt} (cm^2 s^{-1})	D_{tl} (cm^2 s^{-1})	J_∞ (mol cm^{-1} s^{-1})
Type A (5) [a]	$(1.8 \pm 1.7) \times 10^{-8}$	$(2.9 \pm 1.1) \times 10^{-8}$	$(1.5 \pm 0.5) \times 10^{-13}$
Type E (4) [a]	$(2.3 \pm 1.8) \times 10^{-8}$	$(1.1 \pm 0.2) \times 10^{-8}$	$(1.8 \pm 1.2) \times 10^{-13}$

[a] number of tests.

uniformly distributed in the matrix corresponding to a A type microstructure [10]. The second microstructure (Fig. 2(b)) exhibits oriented interdendritic graphite (E type) instead of graphite lamellae as a consequence of a slower cooling rate in some parts of the container. This material appears as substantially free of porosities at the scale of optical microscopy. At higher magnifications a small number of decohesions were observed at the interface between the matrix and the graphite lamellae, presumably as a consequence of the surface preparation.

3.2. Influence of microstructure on hydrogen permeation in 0.1 N NaOH

The hydrogen diffusion coefficient and the permeability to hydrogen measured in 0.1 N NaOH are given in Table 2 as a function of the sample microstructure. Two normalized permeation curves representative of the fastest and slowest hydrogen diffusivity are plotted on Fig. 3 and illustrate the experimental scatter in the time necessary to reach the steady state. Despite the discrepancy of the results given with their standard deviation in Table 2 there is no clear dependence of the permeation characteristics with the microstructure.

The current density corresponding to hydrogen discharged on the input surface at the applied potential of −1350 mV/SCE yields 2.5 mA/cm^2, in agreement with the voltammograms obtained in 0.1 N NaOH (Fig. 4). No significant influence of the microstructure can be detected on this value, nor on the rest potential of the cast iron samples. The corrosion current density computed from Tafel slopes ranges from 1.0 to 10×10^{-7} A cm^{-2} in this medium. These values are in good concordance with the corrosion currents obtained from Tafel slopes on coupons after immersion for two hours in a synthetic solution representative of a concrete water [1]. The general mean corrosion rate of these cast iron samples expressed in terms of thickness loss is lower than 10 μm year^{-1} and decreases with the immersion time due to the formation of $Ca_5SiO_{16}(OH)_2$ or $Ca_5SiO_{17}(OH)_2$ deposits [1].

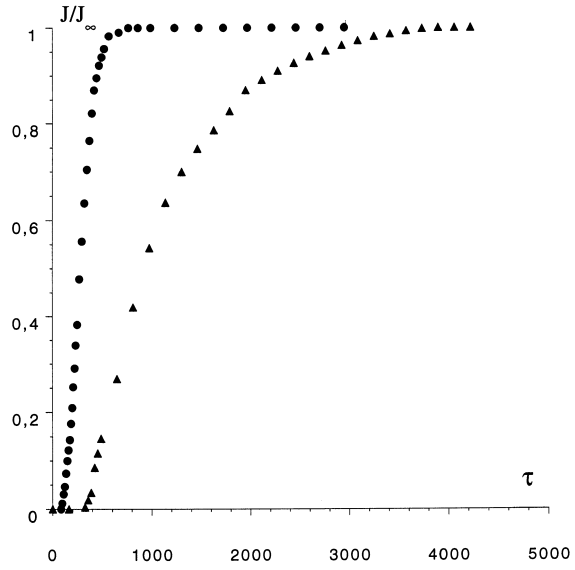

Fig. 3. Permeation curves representative of the largest and smallest diffusivity of hydrogen measured in cast iron (NaOH 0.1 N, −1350 mV/SCE, 298 K).

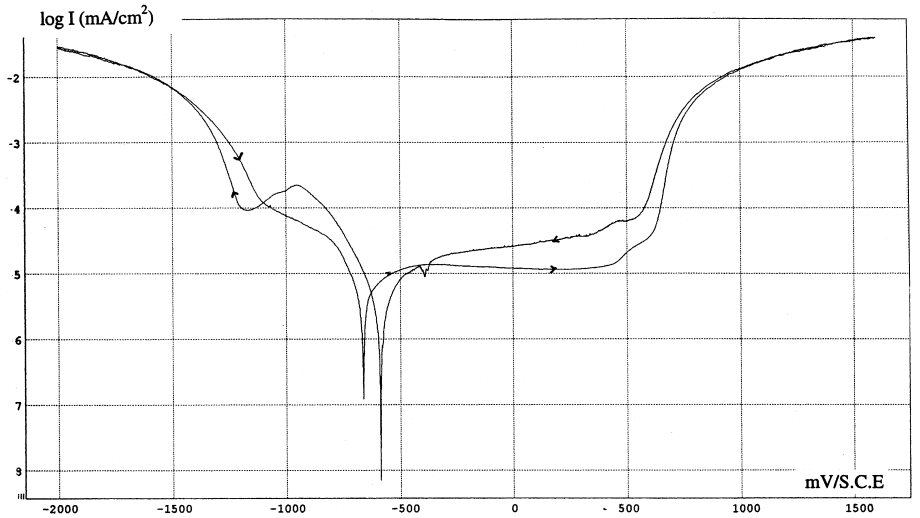

Fig. 4. Cyclic voltammograms recorded on cast iron in 0.1 N NaOH at 298 K.

The comparison of SEM observations performed on the sample surface before and after the permeation tests (Fig. 5) showed for both microstructures a larger number of cracks on cathodically charged samples at the interfaces of graphite clusters or lamellae with the matrix. This may be due to hydrogen trapping at the matrix/graphite interfaces or in preexisting cracks. The large difference in the electrochemical behavior of graphite vs. ferrite may also lead to a localized dissolution of the ferrite. The resulting uncontrollable changes in the surface hydrogen concentration during cathodic charging can explain the experimental scatter.

The diffusion coefficient of hydrogen and the permeability to hydrogen of cast iron are compared in Table 3, for the same charging conditions, with the permeation characteristics of hydrogen at 298 K in a low carbon [11] and a low alloy Cr–Mo steel [12]. As shown by these results, the diffusion coefficient of hydrogen is 10 to 20 times smaller in cast iron than in ferritic steels whereas the permeability to hydrogen of these steels is about two times larger when compared to cast iron.

3.3. Hydrogen degassing

The diffusion coefficient of hydrogen computed from decay transients recorded immediately after stopping the cathodic charging is given in Table 4. The diffusion coefficient computed at the onset of the degassing yields $1-4\times 10^{-7}\mathrm{cm^2s^{-1}}$ and can be considered as the less affected by trapping or surface phenomena at this temperature [13].

The fact that the degassing kinetics assessed with the time lag compares well with the diffusion coefficient calculated with the build up transients (Table 2) indicates that the cracks observed at some graphite/matrix interfaces (Fig. 5) are not high energy trapping sites or that their number is too small to induce a significant decrease in the hydrogen diffusivity. The results of Table 2 and Table 3 are thus in favor of microstructural defects (cementite, graphite, iron nitrides,...) acting as low energy trapping sites for hydrogen in cast iron at 298 K.

3.4. Hydrogen permeation in 0.1 N H_2SO_4

The diffusion curves obtained by cathodic charging in 0.1 N H_2SO_4 lead to a slightly larger (Table 5) value of D_{tl} when compared to the values computed from tests performed in 0.1 N NaOH. This increase in the diffusion coefficient is due to a larger hydrogen activity in acidic

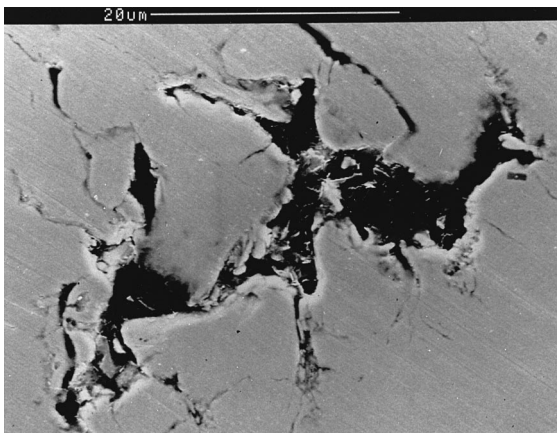

Fig. 5. Optical micrograph showing cracks at graphite clusters in E type cast iron after permeation tests performed in 0.1 N NaOH (−1350 mV/SCE, 298 K).

Table 3
Permeation characteristics of hydrogen in cast iron and in low carbon and low alloy Cr–Mo steels (0.1 N NaOH, −1350 mV/SCE, 298 K)

Material	D_{bt} ($cm^2\ s^{-1}$)	D_{tl} ($cm^2\ s^{-1}$)	J_∞ ($mol\ cm^{-1}.s^{-1}$)
Cast iron type A	$(1.8 \pm 1.7) \times 10^{-8}$	$(2.9 \pm 1.1) \times 10^{-8}$	$(1.5 \pm 0.5) \times 10^{-13}$
Type E	$(2.3 \pm 1.8) \times 10^{-8}$	$(1.1 \pm 0.2) \times 10^{-8}$	$(1.8 \pm 1.2) \times 10^{-13}$
X 65 steel	$(180 \pm 60) \times 10^{-8}$	$(55 \pm 20) \times 10^{-8}$	$(3.9 \pm 0.4) \times 10^{-13}$
Cr–Mo steel	$(61 \pm 5) \times 10^{-8}$	$(53 \pm 9) \times 10^{-8}$	$(3.3 \pm 0.4) \times 10^{-13}$

Table 4
Degassing kinetics of hydrogen after cathodic charging in 0.1 N NaOH (−1350mV/SCE, 298 K)

Microstructure	D_{bt} ($cm^2\ s^{-1}$)	D_{tl} ($cm^2\ s^{-1}$)
Type A (4) [a]	$(25 \pm 14) \times 10^{-8}$	$(2.2 \pm 0.9) \times 10^{-8}$
Type E (4) [a]	$(28 \pm 18) \times 10^{-8}$	$(2.6 \pm 1.7) \times 10^{-8}$

[a] number of tests.

Table 5
Permeation characteristics of hydrogen in cast iron with seldomly oriented graphite lamellae (0.1 N H_2SO_4, −800mV/SCE, 298 K)

Microstructure	D_{bt} ($cm^2 s^{-1}$)	D_{tl} ($cm^2\ s^{-1}$)	J_∞ ($mol\ cm^{-1}\ s^{-1}$)
Type A (3) [a]	$(100 \pm 50) \times 10^{-8}$	$(4.0 \pm 0.7) \times 10^{-8}$	$(6.7 \pm 1.3) \times 10^{-14}$

[a] number of tests.

media and has often been reported for iron and steels [13,14]. The experimental dependency of D with the hydrogen concentration is particularly well illustrated by the 50 fold increase in D_{bt} computed at the onset of the permeation. D_{bt} lies in the range of the highest diffusion coefficients reported in the literature for low carbon steels [15].

The smaller value of the steady state flux of hydrogen in 0.1 N H_2SO_4 can be attributed to the growth of a black deposit on the input surface during cathodic charging in acid. This phenomenon due to the selective dissolution of the ferritic matrix is frequently observed on iron base alloys in acidic media [16,17] and impedes the hydrogen penetration. The thickness of this deposit is large enough to allow EDX analyses after the arrest of cathodic charging. This deposit is made of iron oxide grown on the input surface of cast iron during the permeation test. The oxide accounts for the smaller value of the stationary flux of hydrogen. The large dependence of the diffusion coefficient values with the time chosen in the permeation transient (break-through time or time lag) (Table 5) is another illustration of the increasing barrier effect with time of an oxide film growing on the input surface.

As mentioned in Section 1, the data on hydrogen diffusion in cast iron available from the literature are very scarce. However, permeation experiments conducted under low pressures of gaseous deuterium between 400 and 980 K in cast iron [3] allow a comparison with the present data. Assuming an Arrhenius dependency of D with temperature in the 293–980 K range, the hydrogen diffusivity extrapolated at 298 K (7.3×10^{-10} $cm^2\ s^{-1}$) is about two orders of magnitude smaller than the diffusion coefficient of hydrogen computed with the time lag in this work (Tables 2 and 5). This has to be attributed to the low pressure of deuterium gas [3] and to the dependence of the diffusion coefficient with the hydrogen concentration mentioned here above. The permeability to low pressure of gaseous deuterium measured in [3] is likewise extremely small (about 4 orders of magnitude smaller than the values given in Table 2). The present results obtained in this work by gentle cathodic polarization of cast iron in 0.1 N NaOH are an additional evidence that the permeation characteristics of hydrogen determined by low pressure gas phase experiments cannot be considered as representative of the behavior of hydrogen produced in aqueous media by cathodic or corrosion reactions.

4. Summary

The hydrogen diffusivity in cast iron was computed from permeation experiments conducted on samples exhibiting the two different microstructures encountered in different parts of a container obtained by melting recycled cast iron pieces.

The diffusion coefficient of hydrogen at 298 K ($1–4 \times 10^{-8}$ $cm^2\ s^{-1}$) is much smaller in cast iron than in

ferritic carbon steels for the same electrochemical charging conditions whereas the permeability of cast iron to hydrogen is only two times smaller than the permeability of steels. The diffusion curves obtained by electrochemical charging lead to diffusion coefficient and permeability values markedly larger than the values extrapolated at room temperature from gas phase permeation tests. Cathodic polarization in an acidic solution gives rise to a surface iron oxide which induces a lower permeability to hydrogen.

There is no significant influence of the microstructural characteristics of cast iron on the value of the diffusion coefficient of hydrogen, taking into account the discrepancy in the results which can be attributed to decohesions at the graphite–ferrite interfaces, the number of which increases during cathodic charging. The similarity between the permeation and outgassing kinetics recorded as a function of time after the steady state is reached shows that the microstructural defects in the chosen cast iron samples have a low binding energy with hydrogen at 298 K. The permeation characteristics of hydrogen and the good properties of the recycled cast iron samples regarding the corrosion behavior might lead to foresee a reasonable durability of cast iron containers under subsurface disposal environmental conditions.

Acknowledgements

This work was supported by the 'Commissariat à l'Energie Atomique' (contract n° 2106A063120). Mr Tachon (CEA/UDIN/G2G3) is gratefully acknowledged for the supply of the cast iron samples.

References

[1] M.H. Plouzennec, D. Feron, M. Tachon, R. Atabeck, J. Corcos, Int. Conf. Waste Management 97, March 1997, Tucson, USA.
[2] O.E. Okorafor, C.R. Lopper Jr., Indian J. Technol. 23 (1985) 214.
[3] D. Stöver, H.P. Buchkremer, H.G. Esser, U. Zink, Proc. Int. Conf. Waste Manag., Can. Nucl. Soc., Toronto, Ont. pub., 1982, p. 458.
[4] M.A.V. Devanathan, Z. Stachurski, Proc. Roy. Soc. A 270 (1962) 90.
[5] A.M. Brass, A. Chanfreau, Acta Mater. 9 (1996) 3823.
[6] G.M. Pressouyre, I.M. Bernstein, Acta Metall. 27 (1979) 89.
[7] 38. J. Crank, The Mathematics of Diffusion, Clarendon, Oxford, 1975, p. 326.
[8] J. Mc Breen, L. Nanis, W. Beck, J. Electrochem. Soc. 113 (1966) 1218.
[9] N. Boes, H. Züchner, J. Less Common Met. 49 (1976) 223.
[10] L. Habraken, J.L. de Brouwer, De Ferri Metallographia, Presses Académiques Européennes S.C. Bruxelles, 1966, p. 372.
[11] A.M. Brass, J. Brogan, L. Coudreuse, J.P. Durand, C.Q. Jessen, M. Lamberigts, E. Riecke, L. Scoppio, J.P. Servais. European Commission, Report Eur 16790 EN, Steel Research, 1997, pp. 1–203.
[12] A.M. Brass, J. Collet-Lacoste, M. Garet, J. Gonzalez, La revue de métallurgie-CIT/ Science et génie des Matériaux, 1998, p. 197.
[13] A.M. Brass, J. Collet-Lacoste, Hydrogen Effects in Metals, TMS, 1996, p. 189.
[14] E.G. Daft, K. Bohnenkamp, H.J. Engell, Coros. Sci. 19 (1979) 59.
[15] S.X. Xie, J.P. Hirth, Coros. NACE 38 (1982) 486.
[16] H. Margot-Marette, B. Marandet, J.C. Charbonnier, Mem. Sci. Rev. Met. (1976) 169.
[17] H.W. Pickering, P.J. Byrne, J. Electroc. Soc. 120 (1973) 607.